Load Distribution in Heterogeneous Cellular Networks

Young Jin Sang, *Student Member, IEEE*, and Kwang Soon Kim, *Senior Member, IEEE*

***Abstract*—This letter provides the distributions on the association region of a small-cell BS (sBS) and that of a macro-cell BS (mBS) in a two-tier heterogeneous cellular network (HCN) as functions of the power and density ratios between tiers. Computer simulation results confirm that the proposed distributions are quite accurate for a wide range of network parameters. By using the association region distributions, the load distribution of a BS in each tier is derived. From the results, it is shown that the load is more dispersive in tier s than in tier m, which can be used for devising improved association, resource allocation and load balancing schemes in an HCN.**

***Index Terms*—Heterogeneous cellular network, association region distributions, load distributions.**

I. Introduction

Deployment of small-cell BSs (sBSs) along with existing macro-cell BSs (mBSs) seems to be an attractive solution to handle the tremendous capacity growth driven by the smart mobile devices and an analytical framework for such a heterogeneous cellular network (HCN) in literature greatly improved our understanding for better use of wireless networks [1]-[5]. Assuming Poisson point process (PPP) model for BS locations, it is shown that the distribution of the signal to interference ratio (SIR) of each tier in an HCN is identical to that in a single-tier network [2]. However, the number of associated users to a BS in each tier is quite asymmetric due to the power difference and such an asymmetry brings the necessity for a load balancing in HCN, such as in [6], and the cell range expansion using biasing is considered as a practical technique for offloading the load of high powered mBSs to sBSs [7][8], possibly combined with the use of dedicated resource for sBSs such as in [7]. In such cases, an analytical framework for the number of users associated with a BS or the load requested to a BS is necessary for better understanding on the load balancing in an HCN.

From the PPP modeling of a single-tier cellular network, the association region of a cell forms the well known Poisson Voronoi (PV) tessellation. Even though the exact distribution on the PV size is not yet discovered, there have been efforts for obtaining approximated distributions on the PV size and one promising approach is to use a Gamma distribution [9][10].

Manuscript received September 3, 2013. The associate editor coordinating the review of this letter and approving it for publication was W. Xu.

This work was supported in part by the Basic Science Research Program through the National Research Foundation of Korea funded by the Ministry of Education, Science, and Technology under Grant (No.2013-024473) and in part by the MSIP (Ministry of Science, ICT Future Planning), Korea, under the ITRC (Information Technology Research Center) support program supervised by the NIPA (National IT Industry Promotion Agency) (NIPA-2013-(H0301-13-1005)).

Y. J. Sang and K. S. Kim, corresponding author, are with the Department of Electrical and Electronic Engineering, Yonsei University, 50 Yonsei-ro, Seodaemun-gu, Seoul 120-749, Korea (e-mail: ks.kim@yonsei.ac.kr).

Digital Object Identifier 10.1109/LCOMM.2013.121713.132007

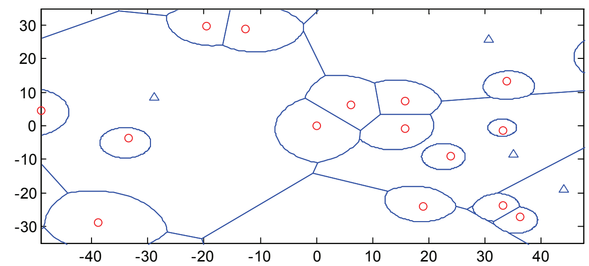

Fig. 1. Weighted PV tessellation of an HCN.

However, the association region of a two-tier HCN is no longer a PV tessellation due to the power difference between tiers. As shown in Fig 1, it becomes a multiplicatively weighted PV tessellation [11], which depends not only on the BS densities but also on the BS powers and the biasing factors. Recently, the distribution on the association area in a two-tier HCN is approximated as that of a single-tier network with each effective density for each tier [11]. However such approximation depends only on the tier association probability so that it does not provide a good approximation when the power difference between tiers is not small.

In this letter, distributions on the association region and the load of a BS in each tier for a two-tier HCN are proposed, which are quite accurate over wide range of density and power differences between tiers.

II. System Model

Consider a two-tier deployment of mBSs and sBSs over a large area where users are uniformly distributed. Here, a user, an mBS and an sBS are respectively denoted by their locations which are respectively given as $\mathbf{u} \in \mathbf{U}$, $\mathbf{x_m} \in \mathbf{X_m}$ and $\mathbf{x}_s \in \mathbf{X}_s$. We assume that mBSs and sBSs are different in terms of transmit power and BS density. The transmit powers of an mBS and an sBS are respectively given as P_m and P_s. Also, mBSs and sBSs are assumed to be randomly distributed according to homogeneous PPPs, Φ_m with density λ_m and Φ_s with density λ_s. We also assume that users are randomly distributed according to a homogeneous PPP, Φ_u with density λ_u. Each user is assumed to be associated with the BS with the highest biased received power. Here, the biased received power is the received power multiplied by each biasing factor (B_m for mBSs and B_s for sBSs). Then, the association region of BS $\mathbf{x}$, $\mathbf{R_x}$, is given as

$$\mathbf{R_x} = \Big\{ \mathbf{y} \in \mathbb{R}^2 \Big| \|\mathbf{y}-\mathbf{x}\| \leq \left(\widehat{P}_{\mathbf{x}}/\widehat{P}_{\bar{\mathbf{x}}}\right)^{\frac{1}{\alpha}} \|\mathbf{y}-\bar{\mathbf{x}}\|, \text{ for all } \bar{\mathbf{x}} \in \mathbf{X}_m \cup \mathbf{X}_s \Big\}, \quad (1)$$

where $\widehat{P}_{\mathbf{x}} = P_{\mathbf{x}} B_{\mathbf{x}}$, $P_{\mathbf{x}} = P_m$ and $B_{\mathbf{x}} = B_m$ if $\mathbf{x} \in \mathbf{X}_m$ and $P_{\mathbf{x}} = P_s$ and $B_{\mathbf{x}} = B_s$ if $\mathbf{x} \in \mathbf{X}_s$, and α denotes the pathloss exponent. Let $A_s = \{\|\mathbf{R}_\mathbf{x}\| | \mathbf{x} \in \mathbf{X}_s\}$ and $A_m = \{\|\mathbf{R}_\mathbf{x}\| | \mathbf{x} \in \mathbf{X}_m\}$ respectively denote the random variables whose realizations are the areas of the association regions in the macro-cell tier (tier m) and the small-cell tier (tier s) having probability density functions (pdfs) of $f_m(x)$ and $f_s(x)$, respectively. Similarly, the number of associated users of a BS in tier j is denoted as N_j ($j \in \{m, s\}$) and the load, or equivalently the number of packet transmission requests per second, for a BS in tier j as L_j ($j \in \{m, s\}$). The probability mass functions (pmfs) of N_j and L_j are respectively denoted as $g_j(k) = \Pr[N_j = k]$ and $l_j(i) = \Pr[L_j = i]$.

III. Load Distributions in a Two Tier HCN

In various work including [9][10], the distribution $f(x; \lambda)$ of the PV tessellation size in a single-tier network can be well approximated by using a Gamma distribution with two parameters, κ_1 and κ_2, as

$$f(x;\lambda) = \frac{(\kappa_1 \lambda)^{\kappa_2}}{\Gamma(\kappa_2)} x^{\kappa_2 - 1} \exp(-\kappa_1 \lambda x), \quad (2)$$

where λ is the BS density, $\Gamma(x) = \int_0^\infty t^{x-1}\exp(-t)dt$ is the Gamma function and the two parameters are given as $\kappa_1 = 3.08$ and $\kappa_2 = 3.04$ [9]. In [10], it is shown that the normalized mean and variance of the above distribution are respectively given as

$$m = \lambda \int_0^\infty x f(x;\lambda)dx \approx 1, \quad (3)$$

$$v = \lambda^2 \int_0^\infty (x - m/\lambda)^2 f(x;\lambda)dx \approx 0.28031. \quad (4)$$

A. Distribution on the association area of an sBS

In [11], the weighted PV of a BS in tier j is approximated as that of a single-tier network, in which the effective density increases $1/p_j$ times (λ_j/p_j), where $p_j = \frac{\lambda_j \widehat{P}_j^{2/\alpha}}{\lambda_m \widehat{P}_m^{2/\alpha} + \lambda_s \widehat{P}_s^{2/\alpha}}$, $j \in \{m, s\}$, denotes the tier j association probability[1]. In [11], the association area of a BS in tier j is assumed to be reduced only by p_j so that it is hard to reflect the effect from the difference in power and density between tiers.

In order to approximate the association area of an sBS better, the nearest cell edge distance is focused in this letter for deriving the effective density. The distribution on the nearest neighboring BS at distance r in a single-tier network is given as $f(r) = 2\pi\lambda r \exp(-\pi\lambda r^2)$ [12]. At a cell edge, the biased received power from the desired BS and the neighboring BS are equal and the nearest cell edge distance s in a single tier network is given as $s = r/2$, which implies that its distribution is given as $f(s) = 8\pi\lambda s \exp(-4\pi\lambda s^2)$. On the other hand, the nearest cell edge distance between an sBS and its nearest mBS at distance r is given as $s = \frac{r}{\bar{P}_r^{1/\alpha}+1}$ due to the power difference, where $\bar{P}_r \left(= \widehat{P}_m/\widehat{P}_s\right)$ denotes the biased power ratio between an mBS and an sBS. Using the superposition property of two independent PPPs, the distribution on the nearest cell edge distance of an sBS, $f_e(s)$, is given as

$$f_e(s) = 8\pi\lambda_e s \exp(-4\pi\lambda_e s^2), \quad (5)$$

[1]It denotes the probability that a randomly selected user is associated with a BS in tier j [2].

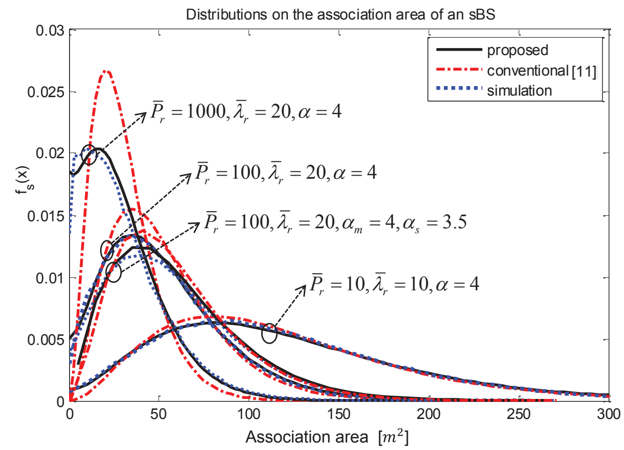

Fig. 2. The distribution on the association area of an sBS.

where $\lambda_e = \lambda_s + \frac{1}{4}\lambda_m \left(1 + \bar{P}_r^{1/\alpha}\right)^2$. As mentioned in [12], the nearest cell edge distance is the key parameter for the distribution on the association area and the distribution on the association area of an sBS may be approximated as that of single-tier network with the effective density of λ_e.

On more thing to consider is that the association area of an sBS is strictly restricted by the nearest mBS [13] and the maximum area of an sBS, when the nearest mBS is located at distance t, is given as $\pi\kappa^2 t^2$, where $\kappa = \frac{\bar{P}_r^{1/\alpha}}{\left|\bar{P}_r^{2/\alpha} - 1\right|}$. Thus, the distribution on the association area of an sBS at a given nearest mBS distance t, $f_s(x|t)$, can be approximated as a truncated distribution using the effective density as

$$f_s(x|t) = f(x;\lambda_e) h(x, \pi\kappa^2 t^2) + F^c(\pi\kappa^2 t^2; \lambda_e)\,\delta(x - \pi\kappa^2 t^2), \quad (6)$$

where $h(x, y) = (u(x) - u(x - y))$, $F^c(x;\lambda) = \int_x^\infty f(t;\lambda)dt$, $u(x)$ denotes the unit step function and $\delta(x)$ denotes the Dirac delta function. Since the distribution of the distance of the nearest mBS is given as $f(t) = 2\pi\lambda_m t \exp(-\pi\lambda_m t^2)$, $f_s(x)$ is obtained as

$$\begin{aligned} f_s(x) &= \int_0^\infty f_s(x|t) f(t) dt \\ &= \exp\left(-\lambda_m \frac{x}{\kappa^2}\right)\left(f(x;\lambda_e) + \frac{\lambda_m}{\kappa^2} F^c(x;\lambda_e)\right) \end{aligned} \quad (7)$$

and the mean and variance of above distribution are respectively denoted as m_s and v_s.

Fig. 2 compares the distributions obtained from (7), that obtained from simulation and that obtained from [11] according to various biased power ratio, $\bar{P}_r$, and density ratio between tiers, $\bar{\lambda}_r = (\lambda_s/\lambda_m)$, when $\lambda_m = 1/800$ (BSs/m^2). For the simulation, 200,000 independent BS realizations are generated for each case to obtain the histogram with bin vector $\mathbf{x} = \left[0, 5, \cdots, \lfloor \frac{4}{5\lambda_e} \rfloor \times 5, \infty\right]$, in which a few thousand realizations per each bin are used in average. From the results, it is confirmed that the proposed distribution is much better matched to the true one while the conventional approximation overestimates it and it becomes severer as the biased power ratio increases.

B. Distribution on the association area of an mBS

In [11], the weighted PV of an mBS is also approximated as that of a single-tier network with the effective density of λ_m/p_m. However, such an approximation only meets the average area of an mBS and it cannot fully reflect the effect caused from difference in power and density between tiers.

First, consider the case where $\bar{P}_r = 1$, which implies that a two-tier HCN becomes a single-tier network with density $\lambda_m + \lambda_s$, where p_m portion of BSs are mBSs and $1-p_m$ portion of BSs are sBSs. Let m_m and v_m respectively denote the mean and variance of the association area of an mBS. Then, $m_m = 1/(\lambda_m+\lambda_s) = p_m/\lambda_m$ and $v_m = 0.28031/(\lambda_m+\lambda_s)^2 = 0.28031 p_m^2/\lambda_m^2$. As $\bar{P}_r$ increases at a given p_m, although m_m does not depend on $\bar{P}_r$ as shown in [11], v_m decreases because larger $\bar{P}_r$ at the same p_m implies $\bar{P}_r^{2/\alpha}$ times more sBSs with smaller sizes and such an improved resolution decreases the size difference among mBSs. Although not shown explicitly, the exponent of p_m in v_m starts at 2 when $\bar{P}_r = 1$ and grows convexly as $\bar{P}_r^{-2/\alpha}$ decreases to zero (i.e., $\bar{P}_r$ increases). By a numerical curve fitting using simulated data similary as in [10], v_m can be approximated as

$$v_m = 0.28031 p_m^{a_1 + a_2\left(\bar{P}_r^{-\frac{2}{\alpha}}\right)^{a_3}}, \tag{8}$$

where $a_1 = 3.8065$, $a_2 = -1.8093$ and $a_3 = 0.2691$.

By adopting a Gamma distribution similarly as in [9][10], $f_m(x)$ can be approximated as

$$f_m(x) = \frac{(\lambda_m \kappa_3)^{\kappa_4}}{\Gamma(\kappa_4)} x^{\kappa_4 - 1} \exp(-\lambda_m \kappa_3 x), \tag{9}$$

where

$$\kappa_3 = \frac{1}{0.28031} p_m^{1-\left(a_1+a_2\left(\bar{P}_r^{-\frac{2}{\alpha}}\right)^{a_3}\right)}, \tag{10}$$

$$\kappa_4 = \frac{1}{0.28031} p_m^{2-\left(a_1+a_2\left(\bar{P}_r^{-\frac{2}{\alpha}}\right)^{a_3}\right)}. \tag{11}$$

Fig. 3 compares the distribution obtained from (9), that obtained from simulation and that obtained from [11] according to various biased power ratio and density ratio between tiers. For the simulation, 200,000 independent BS realizations are generated for each case to obtain the histogram with bin vector $\mathbf{x} = \left[0, 16, \cdots, \lfloor \frac{3p_m}{16\lambda_m} \rfloor \times 16, \infty\right]$, in which a few thousand realizations per each bin are used in average. From the results, it is confirmed that the proposed distribution is much better matched to the true one while the conventional approximation underestimates it and it becomes severer as the biased power ratio increases.

Note that λ_e in (6) can be rewritten as $\lambda_e = \left(16\mathbb{E}^2[s]\right)^{-1}$, where $s = \min\left(\frac{r_s}{2}, \frac{r_m}{\bar{P}_r^{1/\alpha}+1}\right)$ and r_s and r_m respctively denote the nearest distances of the neighboring sBS and mBS. When the pathloss exponents of the two-tiers are different, respectively denoted as α_m and α_s, λ_e can be obtained similarly by using $s = \min(r_s/2, h(r_m))$, where $h(r_m)$ satisfies $P_s h(r_m)^{-\alpha_s} = P_m (r_m - h(r_m))^{-\alpha_m}$. Then, $f_s(s)$ can be numerically obtained by substituting $\pi\kappa^2 t^2$ in (6) with $A(t) = \left\| \left\{ \mathbf{y} \in \mathbb{R}^2 \middle| P_m \|\mathbf{y}\|^{-\alpha_m} \le P_s \|\mathbf{y} - (t,0)\|^{-\alpha_s} \right\} \right\|$.

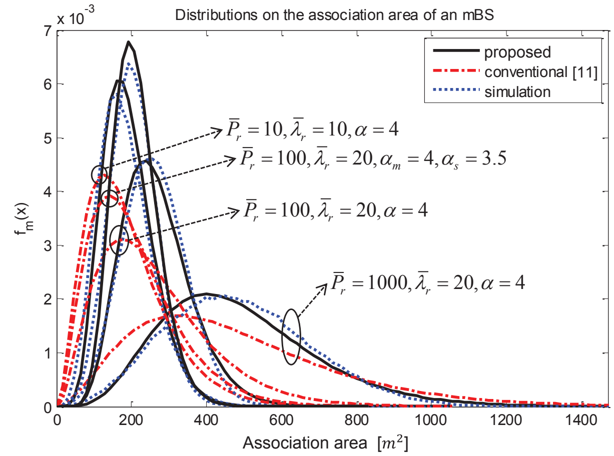

Fig. 3. The distributions on the association area of an mBS.

Also, $f_m(x)$ can be similarly modified by calculating p_m for different pathloss exponents as in [11] and substituting $\bar{P}_r^{2/\alpha}$ with $\bar{P}_r^{2/\alpha_s}$ in (10) and (11). In Figs. 2 and 3, the results for the case are also plotted for confirmation. Thus, although not given as nice closed-forms, the proposed framework can be extended to the case where the pathloss exponents of the two tiers are different. In addition, the proposed framework on the weighted PV tessellation may be useful for applications in various fields such as astrophysics [14].

C. The load distributions

Assume that a user generates a packet transmission request according to an independent and identically distributed (i.i.d) Poisson arrival with arrival rate μ. Then, the pmf of L_j, the number of packet transmission requests per second generated by the associated users of a BS in tier j, is given as

$$l_j(i) = \sum_{k=0}^{\infty} \frac{\exp(-k\mu)(k\mu)^i}{i!} g_j(k), \tag{12}$$

where $g_j(k)$ is the pmf of the number of the associated users with a BS in tier j, which can be obtained as

$$\begin{aligned} g_m(k) &= \int_0^\infty \frac{(\lambda_u x)^k e^{-\lambda_u x}}{k!} f_m(x) dx \\ &= \frac{(n_m/\kappa_3)^k}{(n_m/\kappa_3 + 1)^{k+\kappa_4}} H(k, \kappa_4), \end{aligned} \tag{13}$$

$$\begin{aligned} g_s(k) &= \int_0^\infty \frac{(\lambda_u x)^k e^{-\lambda_u x}}{k!} f_s(x) dx \\ &= H(k, \kappa_2) \left(\frac{\kappa^2}{\kappa^2 (n_s/\kappa_2 + 1) + n_b/\kappa_1} \right)^{k+\kappa_2} \\ &\quad + \frac{(n_s)^k n_b}{\kappa^2 \kappa_1^{k+1}} G(k, \kappa_1, \kappa_2), \end{aligned} \tag{14}$$

where $n_m = \lambda_u/\lambda_m$, $n_s = \lambda_u/\lambda_e$, $n_b = \lambda_m/\lambda_e$, $H(k,a) = \prod_{i=1}^{k} \frac{(k-i+a)}{i}$ and $G(k,b,c) = H(k+1,c)\,{}_2F_1\left[k+1, k+c+1, k+2, -\frac{1}{b}\left(\frac{n_m}{\kappa^2} - n_s\right)\right]$.

In order to obtain some insights on the loads in an HCN from the above distributions, the mean and variance of L_j,

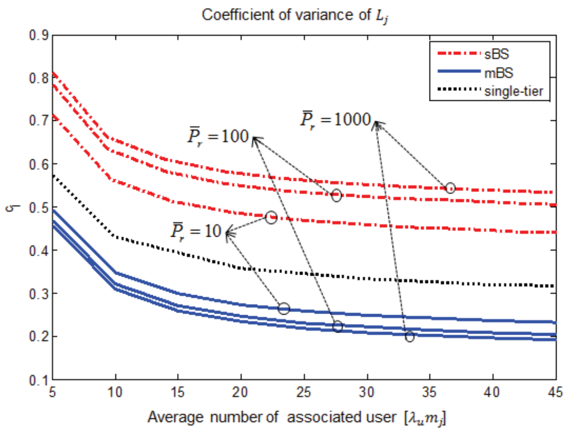

Fig. 4. The coefficient of variance c_j of L_j.

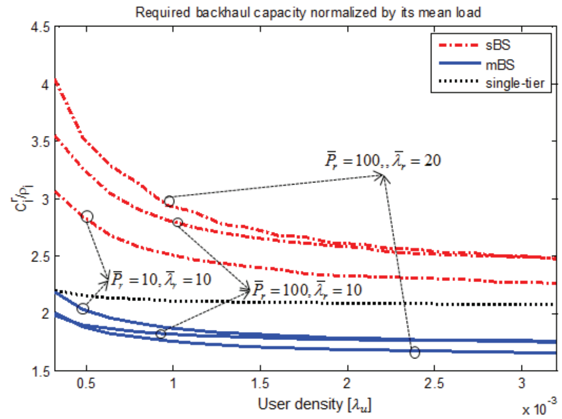

Fig. 5. The normalized required backhaul capacity for a BS in tier j.

respectively denoted as ρ_j and σ_j^2, are obtained by using the law of total variance as

$$\rho_j = \mu \lambda_u m_j, \quad (15)$$
$$\sigma_j^2 = \left(\mu + \mu^2\right) \lambda_u m_j + \mu^2 \lambda_u^2 v_j, \quad (16)$$

and the coefficient of variance of L_j, c_j, is given as

$$c_j = \frac{\sigma_j}{\rho_j} = \sqrt{\frac{(1+\mu)}{\mu \lambda_u m_j} + \frac{v_j}{m_j^2}}. \quad (17)$$

Note that c_j is the measure that quantifies how L_j is dispersed compared to the mean, which implies that a normalized upper quantile of L_j by mean ρ_j increases as c_j increases. Fig. 4 shows c_j according to the mean number of associated users in a BS in tier j ($\lambda_u m_j$) when $p_m = 0.5$ and $\mu = 2$. It is shown in Fig. 4 that c_m is smaller than that of the single-tier network while c_s is larger, and the difference becomes larger as the biased power ratio increases.

As an example of possible applications of the proposed work, a simple HCN design is considered as follows. Consider the case that an operator wants to design the backhaul capacity per BS in tier j, C_j, in order to guarantee the outage probability of the event $L_j > C_j$ below ε for the quality of service (QoS) when $\bar{P}_r$ and $\bar{\lambda}_r$ are already determined for given λ_u and μ. As discussed earlier, the outage probability becomes higher in tier s than in tier m if the backhaul capacity is designed in proportion to its mean load. By using (13) and (14), C_j can be determined to maintain the QoS for each tier. Fig. 5 shows the required backhaul capacity, C_j^r, normalized by its mean load according to the user density of a two-tier HCN when $\varepsilon = 0.05$ and $\mu = 6$.

IV. Conclusion

This letter provides the distributions on the association area of a BS of each tier in a two-tier HCN. The proposed distributions are shown to be quite close to the true distributions over a wide range of network parameters, which would be useful not only for applications in wireless communications but also those related to a weighted PV tessellation.

By using the proposed association region distributions, the load distribution of a BS in each tier in the two-tier HCN is also derived. The proposed load distributions reveal that the load is more dispersive in tier s than in tier m, which can be used for the design of an HCN or devising association, resource allocation and load balancing schemes in an HCN.

References

[1] J. G. Andrews, "Seven ways that HetNets are a cellular paradigm shift," *IEEE Commun. Mag.*, vol. 51, no. 3, pp. 136–144, Mar. 2013.
[2] H.-S. Jo, Y. J. Sang, P. Xing, and J. G. Andrews, "Heterogeneous cellular networks with flexible cell association: a comprehensive downlink sinr analysis," *IEEE Trans. Wireless Commun.*, vol. 11, no. 10, pp. 3484–3495, Oct. 2012.
[3] H. Dhillon, R. Ganti, and J. G. Andrews, "Load-aware modeling and analysis of heterogeneous cellular networks," *IEEE Trans. Wireless Commun.*, vol. 12, no. 4, pp. 1666–1677, Apr. 2013.
[4] X. Lin, J. G. Andrews, and A. Ghosh, "Modeling, analysis and design for carrier aggregation in heterogeneous cellular networks," *IEEE Trans. Commun.*, vol. 61, no. 9, pp. 4002–4015, Sept. 2013.
[5] M. Di Renzo, A. Guidotti, and G. Corazza, "Average rate of downlink heterogeneous cellular networks over generalized fading channels: a stochastic geometry approach," *IEEE Trans. Commun.*, vol. 61, no. 7, pp. 3050–3071, Sept. 2013.
[6] Y. Qiaoyang, B. Rong, Y. Chen, M. Al-Shalash, C. Caramanis, and J. Andrews, "User association for load balancing in heterogeneous cellular networks," *IEEE Trans. Wireless Commun.*, vol. 12, no. 6, pp. 2706–2716, June 2013.
[7] A. Damnjanovic, J. Montojo, Y. Wei, T. Ji, T. Luo, M. Vajapeyam, T. Yoo, O. Song, and D. Malladi, "A survey on 3GPP heterogeneous networks," *IEEE Wireless Commun.*, vol. 18, no. 3, pp. 10–21, June 2011.
[8] B. Bjerke, "LTE-advanced and the evolution of LTE deployments," *IEEE Wireless Commun.*, vol. 18, no. 5, pp. 4–5, Oct. 2011.
[9] H. Hermann, H. Wendrock, and D. Stoyan, "Cell-area distributions of planar voronoi mosaics," *Metallography*, vol. 23, no. 3, pp. 189–200, Dec. 1989.
[10] M. Tanemura, "Statistical distributions of poisson voronoi cells in two and three dimensions," *Forma*, vol. 18, no. 4, pp. 221–247, Nov. 2003.
[11] S. Singh, H. Dhillon, and J. G. Andrews, "Offloading in heterogeneous networks: modeling, analysis, and design insights," *IEEE Trans. Wireless Commun.*, vol. 12, no. 5, pp. 2484–2497, May 2013.
[12] D.Weaire, J. P. Kermode, and J. Wejchert, "On the distribution of cell areas in a voronoi network," *Philos. Mag. Part B*, vol. 53, no. 5, pp. L101–L105, May 1986.
[13] H.-S. Jo, P. Xia, and J. G. Andrews, "Open, closed, and shared access femtocells in the downlink," *EURASIP J. Wireless Commun. and Netw.*, vol. 2012, no. 1, pp. 1–16, Dec. 2012.
[14] C. J. Schrijver, J. H. Hagenaar, and M. Alan, 'On the patterns of the solar granulation and supergranulation," *Astrophy. J.*, vol. 475, no. 1, pp. 328–337, Jan. 1997.